Results in Engineering 18 (2023) 101117

Contents lists available at ScienceDirect

Results in Engineering

journal homepage: www.sciencedirect.com/journal/results-in-engineering

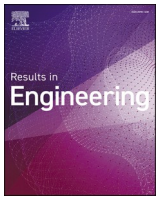

Development of a methodology for mechanical testing of steel samples for predicting the durability of vehicle wheel rims

S. Belodedenko [a], O. Hrechanyi [b,*], T. Vasilchenko [b], K. Baiul [a,c], A. Hrechana [d]

[a] Department of Industrial Machinery Engineering, Ukrainian State University of Science and Technologies, Dnipro, Ukraine
[b] Department of Metallurgical Equipment, Zaporizhzhia National University, Zaporizhzhia, Ukraine
[c] Department of Technologica Equipment & Control System, Z.I. Nekrasov Iron and Steel Institute, National Academy of Sciences of Ukraine, Dnipro, Ukraine
[d] Master of Law, National Technical University of Ukraine "Igor Sikorsky Kyiv Polytechnic Institute", Kyiv, Ukraine

ARTICLE INFO

Keywords:
Impact Strength
Stresses
Fatigue crack
Wheel
Testing

ABSTRACT

The reliability and durability of parts of aggregates and mechanisms of motor vehicles depend on the efficiency of the basic and responsible load-bearing structures. The responsible elements of the motor vehicle are the wheel rims, whose reliability will increase the energy efficiency of the motor vehicle as a whole. One of the directions for increasing the reliability of wheel rims is the use of optimized low-pearlite steels with the increased impact strength of the 10HFTBch type. When determining the mechanical characteristics of steels with increased impact strength, it is worth considering a mixed form of failure; therefore, the scheme of four-point asymmetric bending is optimal for laboratory research. Conditions of mixed failure for an oblique crack lead to a 25–45% decrease in the value of ΔK_{Im}* relatively to the stress intensity factor ΔK_I* obtained for the pure I mode. The same can be said about the II mode, when ΔK_{II}* determined during the growth of an oblique crack is 10% smaller than the value of ΔK_{II}*, which is calculated for the pure mode of failure, This indicates an increase in the fatigue crack growth rate for mixed failure compared to pure modes.

1. Introduction

The reliability and durability of motor vehicle parts, like other products, depend on the performance of the basic and responsible load-bearing structures [1,2]. So, for example, the wheel rims of trucks are a responsible part because they are one of the most loaded, and their failure leads to losses that significantly exceed the cost of the unit itself [3]. Therefore, the production of wheels with an increased energy load will allow not only to increase the mass of transported cargo several times under the existing operating conditions, but also to reduce fuel consumption due to a reduction in the number of flights [4,5].

The problem of increasing the load capacity of car wheels while simultaneously reducing their weight is an old one. Solution to this problem using technological means (in particular, the use of high-strength sheet manganese steels made by hot stamping) started in the last century [6]. At the current stage of wheel manufacturing, experts are actively introducing new alloys with high specific strengths [7,8]. Apart from reducing the mass, the wheel becomes corrosion-resistant [9–11]. But replacing such wheels for trucks is risky.

Reliability of wheels is ensured by calculating their elements for strength while designing them. Currently, FEM programs are widely used, which allow making multivariate calculations where the complex stress state of the metal is taken into account through equivalent normal stresses [6,8,12]. Performance testing is carried out on special test stands, where standard and emergency situations are simulated [9,13]. Endurance resource tests can also be carried out on these stands. But due to complex damage, the test results are in a wide range, which makes it difficult to draw conclusions. Therefore, preference should be given to multi-sample test methods when they simulate the stressed state of the material in the wheel.

Wheel rims of trucks operate under conditions of cyclic shock loading, which over time leads to the formation of fatigue cracks [14]. Further transformation of the crack into the main one is possible in several directions. Depending on this, crack growth can accelerate or

Abbreviations: KCU, impact strength (MJ/m2); SIF, stress intensity factor (MPa$\sqrt{M}$); 4PAB, four-point asymmetric bending; l, sample length (mm); b, sample width (mm); h, sample height (mm); a_0, a_c, fatigue crack length (mm); ε, relative crack length; σ, normal stresses (MPa); τ, shear stresses (MPa); N_g, number of cycles; FCG, fatigue crack growth; γ_{lb}, arm coefficient.

* Corresponding author.
E-mail address: hrechanyi@znu.edu.ua (O. Hrechanyi).

https://doi.org/10.1016/j.rineng.2023.101117
Received 24 March 2023; Received in revised form 16 April 2023; Accepted 20 April 2023
Available online 24 April 2023

slow down. Therefore, a significant period of rims' durability is accompanied by the development of cracks [13]. If the direction of development of cracks varies during maintenance, then the source of their appearance is almost always near the mounting hole under the washer of the bolted connection. Then it is clear that fretting processes significantly affect the formation and growth of cracks [15].

It is known that II mode deformations are responsible for the initiation of destruction during contact (in particular, fretting fatigue) [16,17]. Knowledge of standard material properties is not enough to assess the conditions for the genesis of a crack. It is necessary to have the parameters of the kinetic diagram of internal destruction (Peris diagrams) for the II mode. Greater crack development occurs in conditions of mixed failure, when detachment mechanisms begin to act (I mode). To predict survivability (the number of crack growth cycles to the critical size) in such conditions, the method of pure modes has been developed [18]. It is based on the construction of survivability curves, which allows to predict the lifetime under non-stationary complex loading.

The development of technology and the implementation of scientific achievements contribute to the creation of new materials [19,20]. One of the ways to increase the reliability of wheel rims is to replace the low-carbon steel 15 widely used in their production with optimized low-pearlite steels with increased impact strength KCU, which includes steel 10HFTBch (KCU = 0,80 MJ/m^2) [21].

After establishing the influence of the main technological factors on the quality of the newly developed 10HFTBch steel, the issue of developing a test scheme to determine its service characteristics arises [22,23]. Such characteristics make it possible to predict the durability of the rim at various stages of operation [24–28].

To simulate the conditions of deformation in the II mode, the scheme of four-point asymmetric bending (4PAB) has become widespread. For its implementation, it allows the use of universal testing machines and simple samples. This scheme is well combined with the three-point bending scheme, in which parameters of fatigue failure at the I mode are obtained. The 4PAB scheme is well established for elastic-brittle materials when the failure of the sample is a direct crack under the load support. For such conditions, formulas for calculating stresses and the stress intensity factor (SIF) for a straight crack are defined. Structural elastic-plastic materials, in particular, wheel steels, are destroyed by an oblique fracture. So with the development of an oblique crack, which indicates a mixed nature of destruction. For such conditions, there are no reasonable dependencies for determining SIF. This makes it impossible to obtain fatigue failure diagrams.

The purpose of these studies was to develop a methodology for testing steel samples according to the 4PAB scheme, at which it is possible to obtain parameters of fatigue failure. In turn, such parameters should be sufficient to use the method of "pure" modes to predict survivability in case of mixed destruction.

2. Materials and methods

2.1. Samples and equipment for testing

The research was carried out by testing samples under 4PAB. This method of research has proven its effectiveness in determining the parameters of mixed destruction [18].

Samples for bending have the form of a bar with a rectangular cross-section. Their length is l = 120 mm, width – b = 5 mm, height – h = 20 mm. In the samples, in the middle, to initiate the crack, a U-shaped incision on the edge with a depth of 5 mm was made, and therefore the stress concentration coefficient α_σ>>1.

Samples are made of 9XC(9HS) (analogy 90CrSi5) steel with impact strength KCU = 0.78 MJ/m^2, which is close to the microalloyed steel with increased impact strength proposed in the work [21].

Cyclic loading tests were carried out on a universal machine with a hydropulsator.

The appearance of a crack was recorded visually. Sign-invariant

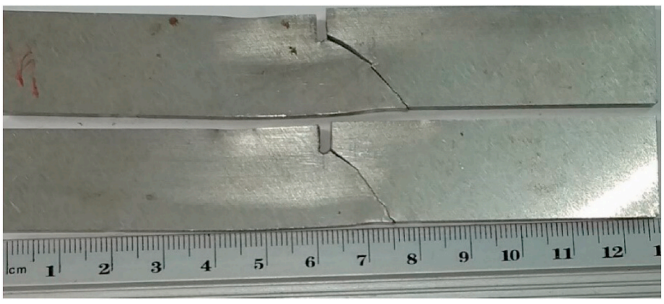

Fig. 1. The location of an oblique crack in the 4PAB deformation scheme.

modes were used, in which the minimum force was 4 kN. Cycle asymmetry coefficient is 0.10 ÷ 0.30. Frequency of cyclic stresses: 10–15 Hz. A higher frequency was intended for the crack initiation stage. After the appearance of the crack, the frequency decreased.

2.2. Methodology for processing the results of mechanical tests

There are different solutions for determining the stress intensity factor (SIF) during tests. Depending on the factors of influence, the range of their changes for $K_I = 1 \div 4{,}49$, for $K_{II} = 1 \div 3{,}03$ [29,30].

The biggest difference when using different formulas is observed, as a rule, at the extreme values of the factors, for example, at the relative length of the crack $\varepsilon = a/h > 0{,}7$. Obviously, the first solution for the 4PAB scheme was proposed in 1987 by Y. Murakami [31]:

$$K_I = \sigma F_1 \sqrt{\pi a}, K_{II} = \tau F_{1I} \sqrt{h}. \quad (1)$$

Geometric functions $F_{I(II)}$ depend on the relative length and are approximated by polynomials:

$$F_I = 1,21\varepsilon + 3,74\varepsilon^2 + 3,87\varepsilon^3 - 19,05\varepsilon^4 + 22,55\varepsilon^5 \quad (2)$$

$$F_{II} = 7,26 - 9,73\varepsilon + 2,74\varepsilon^2 + 1,87\varepsilon^3 - 1,04\varepsilon^4 \quad (3)$$

Function F_{II} is monotonically decreasing and function F_I is increasing.

Further solution (1) was modified [32]:

$$K_{II} = \tau F_{1I} \frac{\varepsilon^{1.5}}{\sqrt{1-\varepsilon}} \sqrt{h} \quad (4)$$

In addition, Fett's corrections for the displacement of the crack from the median plane are known [33]. Taking them into account (4) is transformed as:

$$K_{II} = \tau F_{1I} \frac{\varepsilon^{1.5}}{\sqrt{1-\varepsilon}} \left(1 - \frac{x}{L_2}\right) \sqrt{h} \quad (5)$$

For K_I such correction is unnecessary, since the displacement x is taken into account when determining the bending moment M.

To establish the kinetics of crack growth based on test results, using the previously established formulas (1.7)–(1.9) in work [18] for samples with a height of h = 20 mm, we obtain simplified formulas for the number of cycles to crack growth from the size a_0 (ε_0) to the size a_c (ε_c):

$$N_{gI} = 1.5 \cdot 10^7 \left(\frac{\Delta K_I^*}{1.65 \cdot \Delta\sigma}\right)^4 [\exp(-13.36\varepsilon_0) - \exp(-13.36\varepsilon_c)] \quad (6)$$

$$N_{gII} = 5 \cdot 10^6 \left(\frac{0.043 \cdot \Delta K_{II}^*}{\Delta\tau}\right)^4 \left(\frac{1}{(a_0 - 0.0005)^2} - \frac{1}{(a_c - 0.0005)^2}\right) \quad (7)$$

3. Results and discussion

The crack grew almost immediately from the cut at the deviation angle θ towards the zone of tensile stresses caused by bending (Fig. 1).

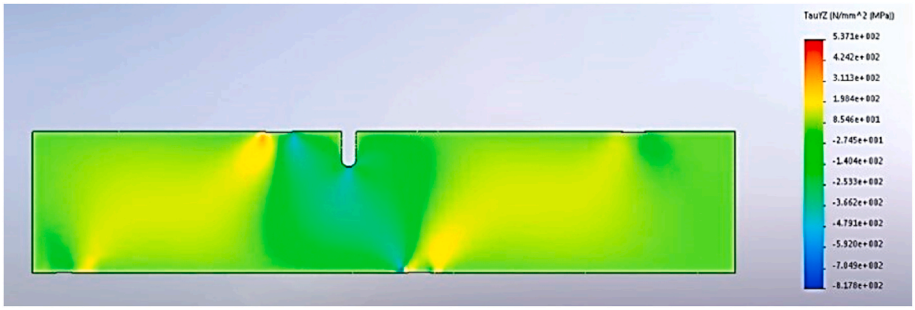

Fig. 2. Fields of tangential stresses in the sample with the 4PAB deformation scheme.

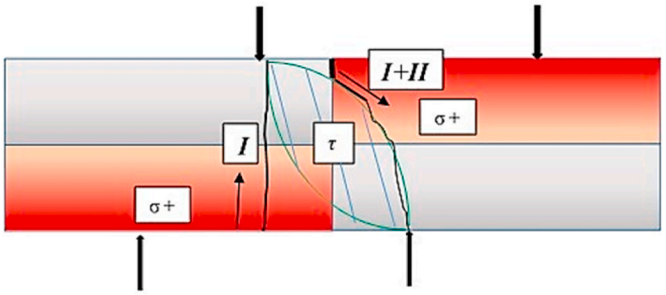

Fig. 3. Schemes of the development of cracks in the samples with the 4PAB deformation scheme.

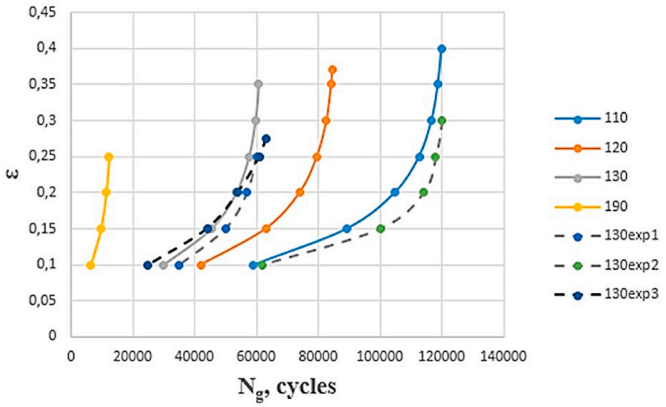

Fig. 4. Kinetics of a straight crack growth in 9XS steel samples during four-point bending for the range of shear stresses Δτ = 110, 120, 130, 190 MPa (model curves – solid line, experimental – dotted line).

The breaking of the sample occurs in the direction of the support. Such a crack trajectory is typical for tests of metals in this scheme and indicates a mixed I + II mode [34].

Although there are no bending moments in the middle section that provoke the destruction of the I mode, they are present from the very beginning of the appearance of the crack. In our opinion, the origin of the I-mode fractures here is due to the inaccuracy of the sample installation (from Fig. 1 it is clear that the crack does not originate from the root of the cut), as well as friction of the crack edges. This indicates the influence of the factor of mixed destruction.

In the research [18] part of the samples that were tested according to the 4PAB scheme broke into three parts due to an additional fracture by the I mode. This situation arose as a result of insufficient cutting sharpness and low concentration of tangential stresses. This is evidenced by the finite-elemental analysis of the stressed state of the sample (Fig. 2).

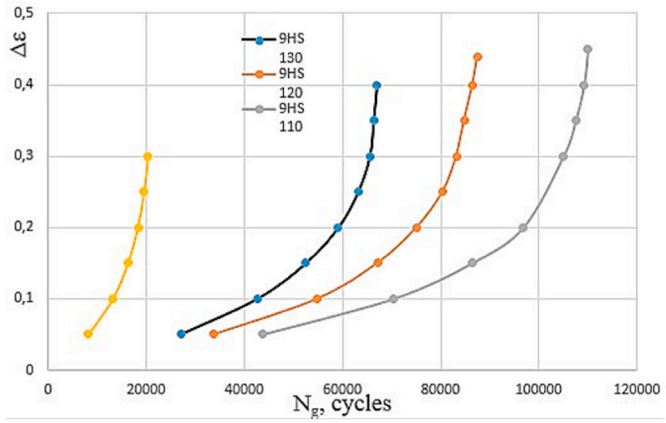

Fig. 5. Comparative graphs of oblique crack growth in 9XC steel samples, obtained by models for the range of shear stresses Δτ = 110, 120, 130, 190 MPa.

Table 1
Experimental indices of cyclic fracture toughness.

№	Scheme	Shape of the crack trajectory	Mode	Indicator designation, MPa$\sqrt{M}$	9XC steel
1	4PAB	straight	I	ΔK_I*	43
2	4PAB	oblique	I+II	ΔK_{Ilm}*	35
				ΔK_{IIlim}*	18
				ΔK_{eff}*	49

Scheme of the development of the sample's destruction was made (Fig. 3) on the basis of the finite-elemental analysis, fatigue tests and work results [18]. If the oblique crack grows from the cut, then the straight crack begins on the opposite side of the sample opposite the support (I, Fig. 3). The maximum tensile stresses are marked in the form of red zones. The growth of oblique and straight cracks occurs in opposite directions.

Thus, at a four-point bend, the fracture parameters were obtained for an oblique (mixed I + II fracture) and direct (I mode) crack.

Original curves of fatigue crack growth (FCG) were obtained experimentally in the form of graphs of crack length a – number of cycles N_g.

In the future, relative length was used instead of absolute length ε (smooth samples) or $\Delta\varepsilon=(a-a_0)/h$ (samples with a cut depth a_0) (Figs. 4 and 5).

Along with experimental curves, model curves were obtained by the developed algorithm FCG (Figs. 4–5). They are based on value $\Delta K^*_{I(II)}$, obtaining which is the main result of fatigue tests (Table 1). For mixed destruction I + II, the effective value is given SIF ΔK^*_{I+II}, which is obtained by Richard's criteria. It is chosen as the one that maximally "enhances" the effect of the II mode.

The tendency of the deterioration of the resistance to destruction with the 4PAB-scheme tests in the conditions of straight cracks was confirmed. For them the value of ΔK* is 25–45% smaller than the pure ΔKI*, obtained according to the 3PB-scheme. This leads to an increase in the speed of FCG by 2.5–4.5 times, which leads to a decrease in durability and survivability.

The deterioration of the resistance in the cyclic process in the conditions of the I mode for the 4PAB scheme is explained by the increase in the contribution of tangential shear stresses. In the case of transverse bending, theoretically, there is a section in which there are no shear deformations. However, their sharp spike occurs in the surrounding areas. This circumstance affects the intensity of FCG.

The contribution of tangential stresses is estimated through the lever arm coefficient [18] $\gamma_{lb} = \sigma/(\tau k_f)$ where the coefficient of the cross-sectional shape k_f is constant for structural element. Decrease of the lever arm coefficient γ_{lb} indicates an increase in the contribution of shear stress and destruction of the II mode or an increase in the effective ratio K_{II}/K_I.

The factor γ_{lb} has a contradictory effect on the fatigue resistance of materials. At the stage of crack initiation, its reduction leads to an increase in the cyclic strength and durability of N [35]. At the stage of crack growth, increase in factor γ_{lb} leads to an increase in speed of FCG and, as a result, a decrease in value ΔK_I^*. Such ambiguous effects are not unique to combined load conditions. For example, torque (III mode) reduces the cyclic strength of shafts loaded by bending with rotation (I mode). However, when the crack reaches a certain length, the appearance of the III mode helps to slow down its development [36].

4. Conclusions

A test method was developed according to the 4PAB scheme, which includes the shape and dimensions of the samples, the scheme of their installation relatively to the supports, dependencies for calculating stresses and SIF. The latter are original.

Mixed failure conditions for an oblique crack leads to a 25–45% decrease in value ΔK_{Im}^* relatively SIF ΔK_I^*, obtained for pure I mode. The same can be said about the II mode, when ΔK_{IIm}^* determined during the growth of an oblique crack is 10% smaller than the value of ΔK_{II}^*, which is calculated for the pure failure mode. But difference between these indicators (i.e. $\Delta K_{IIm}^* - \Delta K_{II}^*$) is much smaller, than difference between SIF of I mode $\Delta K_{Im}^* - \Delta K_{Im}^*$. I.e.:/$\Delta K_{IIm}^* - \Delta K_{II}^*$/</$\Delta K_{Im}^* - \Delta K_{Im}^*$/. All this indicates an increase in speed of FCG for mixed failure versus pure modes.

Declaration of competing interest

The authors declare that they have no known competing financial interests or personal relationships that could have appeared to influence the work reported in this paper.

Data availability

Data will be made available on request.

References

[1] S. Belodedenko, O. Hrechanyi, V. Hanush, A. Vlasov, Estimating the residual resource of basic structures using a model of fatigue durability under complex loading, E. Eur. J. Enterprise Technol. 3 (117) (2022) 33–41, https://doi.org/10.15587/1729-4061.2022.257013.

[2] S.V. Belodedenko, G.M. Bilichenko, O.M. Hrechanyi, M.S. Ibragimov, Application of risk-analysis methods in the maintenance of industrial equipment, Procedia Struct. Integr. 22 (2019) 51–58, https://doi.org/10.1016/j.prostr.2020.01.007.

[3] O.O. Shapurov, State and trends of machine-building development, Actual Probl. Econ. 3 (2009) 57–63.

[4] M. Tryputen, V. Kuznetsov, M. Kovzel, V. Kovalenko, V. Artemchuk, V. Nadtochyi, Minimization of the description of images in the problem of adaptive control of static technological objects, in: 2021 IEEE International Conference on Modern Electrical and Energy Systems, MEES, Kremenchuk, Ukraine, 2021, pp. 1–4, https://doi.org/10.1109/MEES52427.2021.9598651.

[5] S. Sheyko, V. Tsyganov, O. Hrechanyi, T. Vasilchenko, A. Vlasov, Mechanical property investigation of welded joints in 10HFTBch steel for the automobile wheel production, Mater. Lett. X 17 (2023), 100181, https://doi.org/10.1016/j.mlblux.2023.100181.

[6] G. Marron, P. Teracher, The application of high-strength, hot-rolled steels in auto wheels, JOM 48 (1996) 16–20, https://doi.org/10.1007/BF03222988.

[7] Y. Belokon, O. Hrechanyi, T. Vasilchenko, D. Krugliak, Y. Bondarenko, Development of new composite materials based on TiN–Ni cermets during thermochemical pressing, Results Eng. 16 (2022), 100724, https://doi.org/10.1016/j.rineng.2022.100724.

[8] C.Y. Loi, H.Y. Choy, Modelling and fatigue analysis of automobile wheel rim, in: 5th International Conference on Control, Automation and Robotics, ICCAR, Beijing, China, 2019, pp. 696–701, https://doi.org/10.1109/ICCAR.2019.8813410.

[9] Qian Gao, Yingchun Shan, Xiaofei Wan, Qizhang Feng, Xiandong Liu, 90-degree impact bench test and simulation analysis of automotive steel wheel, Eng. Fail. Anal. 105 (2019) 143–155, https://doi.org/10.1016/j.engfailanal.2019.06.097.

[10] Hasan Köten, Advanced numerical and experimental studies on ci engine emissions, J. Therm. Eng. 4 (2018) 2234–2247, https://doi.org/10.18186/journal-of-thermal-engineering.434044.

[11] Hasan Koten, Ozge Kamaci, Time-dependent corrosion resistance investigation of hydrophobic magnesium alloys, Adv. Mater. Sci. Eng. (2023) 281–292, https://doi.org/10.1007/978-981-19-3307-3_24.

[12] Lehar Asip Khan, Eanna McCarthy, Corné Muilwijk, Inam Ul Ahad, Dermot Brabazon, Analysis of nitinol actuator response under controlled conductive heating regimes, Results Eng. 18 (2023), 101047, https://doi.org/10.1016/j.rineng.2023.101047.

[13] G.V. Tsybanev, S.L. Ponomarev, Fatigue of low-carbon and low-alloyed steels for the automotive industry. Part 1. The influence of stress concentration and fretting on fatigue life of full-scale automobile wheels and specimens, Strength Mater. 33 (2001) 8–14, https://doi.org/10.1023/a:1010455025000.

[14] L.V. Agamirov, A.N. Lisin, V.V. Mozalev, Integrated prognostication esistance automobile wheel fatigue and skew blow, Automot. Indus. 10 (2011) 17–21.

[15] Z. Zheng, S. Yuan, T. Sun, S. Pan, Fractographic study of fatigue cracks in a steel car wheel, Eng. Fail. Anal. 47 (2015) 199–207, https://doi.org/10.1016/j.engfailanal.2014.09.010.

[16] Y. Murakami, C. Sakae, S. Hamada, Mechanism of Rolling Contact Fatigue and Measurement of ΔK_{IIth} for Steels. Engineering against fatigue, 1999, pp. 473–485.

[17] O. Datsyshyn, V. Panasyuk, Structural Integrity Assessment of Engineering Components under Cyclic Contact, Springer International Publishing, 2020, p. 325, https://doi.org/10.1007/978-3-030-23069-2.

[18] S.V. Belodedenko, V.I. Hanush, O.M. Hrechanyi, Experimental verification of the survivability model under mixed I+II mode fracture for steels of rolling rolls, Struct. Integr. 25 (2022) 3–12, https://doi.org/10.1007/978-3-030-91847-7_1.

[19] Makarim A. Mahdi, Seyede Raheleh Yousefi, Layth S. Jasim, Masoud Salavati-Niasari, Green synthesis of DyBa2Fe3O7.988/DyFeO3 nanocomposites using almond extract with dual eco-friendly applications: photocatalytic and antibacterial activities, Int. J. Hydrogen Energy 47 (2022) 14319–14330, https://doi.org/10.1016/j.ijhydene.2022.02.175.

[20] Seyede Raheleh Yousefi, Hassan Abbas Alshamsi, Omid Amiri, Masoud Salavati-Niasari, Synthesis, characterization and application of Co/Co3O4 nanocomposites as an effective photocatalyst for discoloration of organic dye contaminants in wastewater and antibacterial properties, J. Mol. Liq. 337 (2021), 116405, https://doi.org/10.1016/j.molliq.2021.116405.

[21] Patent No. 105341 Ukraine, IPC C22C38/28 (2006.01), Low- Alloyed Steel, Bull, 2014, p. 5. V.G. Mishchenko, S.B. Belikov, S.P. Sheyko and Others - Publ 8.

[22] V.A. Noskov, K.V. Bayul, Research of influencing of configuration of shaping elements on the tensely-deformed state and parameters of compression of fine-fractional charge, Metallurgicheskaya i Gornorudnaya Promyshlennost 2 (2005) 104–108.

[23] B. Sereda, Y. Belokon, S. Sheyko, D. Sereda, The research of influence alloying elements on processes structure formation in stamp steel, in: AIST Steel Properties and Applications Conference Proceedings, 2012, pp. 453–456.

[24] A. Naim, R. Kumar, S. Bhatia, A review paper on materials used for manufacturing of alloy wheels, IOP Conf. Ser. Mater. Sci. Eng. 1136 (1) (2021), 012006, https://doi.org/10.1088/1757-899x/1136/1/012006.

[25] X. Liu, Y. Qu, X. Yang, Y. Shen, Load spectrum compiling and fatigue life estimation of the automobile wheel hub, Recent Pat. Mech. Eng. 13 (2020) (2021) 366–379, https://doi.org/10.2174/2212797613999201231200939.

[26] Y. Zhao, et al., A fabrication history based strain-fatigue model for prediction of crack initiation in a radial loading wheel, Fatig. Fract. Eng. Mater. Struct. 40 (11) (2017) 1882–1892, https://doi.org/10.1111/ffe.12607.

[27] B. Sereda, I. Kruglyak, A. Kovalenko, D. Sereda, T. Vasilchenko, The deformation zone geometrical factors and its influence on deformation shift degree for the axial zone of rolled high bars, Metall. Min. Ind. 3 (7) (2011) 102–106.

[28] M. Mihaliková, A. Lišková, A. Kovalčíková, та J. Micheľ, The analysis of automotive steels at different strain rate, Mater. Today: Proc. 3 (4) (2016) 1064–1068, https://doi.org/10.1016/j.matpr.2016.03.049.

[29] R. Ravichandaran, G. Thanigaiyarasu, Mixed-mode fracture analysis of aluminum alloy 5083 subjected to four point bending, J. Appl. Sci. 11 (2011) 2214–2219, https://doi.org/10.3923/jas.2011.2214.2219.

[30] E.A. Zimmermann, M.E. Launey, R.O. Ritchie, The significance of crack-resistance curves to the mixed-mode fracture toughness of human cortical bone, Biomaterials 31 (20) (2010) 5297–5305, https://doi.org/10.1016/j.biomaterials.2010.03.056.

[31] Y. Murakami, Stress Intensity Factors Handbook, Pergamon, Oxford, 1987, 0080348092.
[32] M.Y. He, J.W. Hutchinson, Asymmetric four-point crack, J. Appl. Mech. 67 (1) (2000) 207–209, https://doi.org/10.1115/1.321168.
[33] T. Fett, Stress Intensity Factors and Weight Functions for Special Crack Problems, Forschungszentrum Karlsruhe GmbH, Karlsruhe, 1998, p. 36.
[34] Sérgio Gonçalves Pereira, Sérgio Tavares, та Paulo de Castro, Mixed mode fracture: numerical evaluation and experimental validation using PMMA specimens, Frat. Ed. Integrità Strutt. 13 (49) (2019) 412–428, https://doi.org/10.3221/igf-esis.49.40.
[35] S. Belodedenko, A. Grechany, A. Yatsuba, Prediction of operability of the plate rolling rolls based on the mixed fracture mechanism, E. Eur. J. Enterprise Technol. 1 (91) (2018) 4–11, https://doi.org/10.15587/1729-4061.2018.122818, 7.
[36] M. Da Fonte, L. Reis, M. De Freitas, The effect of steady torsion on fatigue crack growth under rotating bending loading on aluminium alloy 7075-T6, Frat. Ed. Integrità Strutt. 8 (30) (2014) 360–368. https://doi:10.3221/igf-esis.30.43.